Carbohydrate Polymers 271 (2021) 118429

Contents lists available at ScienceDirect

Carbohydrate Polymers

journal homepage: www.elsevier.com/locate/carbpol

Impact of heterogeneously crosslinked calcium alginate networks on the encapsulation of β-carotene-loaded beads

Joel Girón-Hernández [a], Piergiorgio Gentile [b], María Benlloch-Tinoco [c,*]

[a] Universidad Surcolombiana, Departamento de Ingeniería Agrícola, Avenida Pastrana Borrero – Carrera 1, Neiva 410007, Colombia
[b] Newcastle University, School of Engineering, Claremont Road, Newcastle upon Tyne NE1 7RU, United Kingdom
[c] Northumbria University, Department of Applied Sciences, Faculty of Health and Life Sciences, Ellison Place, Newcastle upon Tyne NE1 8ST, United Kingdom

ARTICLE INFO

Keywords:
Calcium alginate networks
Heterogeneity crosslinking
Encapsulation
Barrier properties
Mechanical properties
β-Carotene

ABSTRACT

This study investigated the impact of heterogeneity of crosslinking on a range of physical and mechanical properties of calcium alginate networks formed via external gelation with 0.25–2% sodium alginate and 2.5 and 5% $CaCl_2$. Crosslinking in films with 1–2% alginate was highly heterogeneous, as indicated by their lower calcium content (35–7 mg Ca·g alginate^{-1}) and apparent solubility (5–6%). Overall, films with 1–2% alginate showed higher resistance (tensile strength = 51–147 MPa) but lower elasticity (Elastic Modulus = 2136–10,079 MPa) than other samples more homogeneous in nature (0.5% alginate, Elastic Modulus = 1918 MPa). Beads with 0.5% alginate prevented the degradation of β-carotene 1.5 times more efficiently than 1% beads (5% $CaCl_2$) at any of the storage temperatures studied. Therefore, it was postulated that calcium alginate networks crosslinked to a greater extent and in a more homogeneous manner showed better mechanical performance and barrier properties for encapsulation applications.

1. Introduction

Alginate is a natural ionic polysaccharide that finds countless applications in a range of life-science related environments, like thickener and stabilizer in foods and beverages or encapsulating material for living cells (Chan et al., 2006). Indeed, the attractiveness and versatility of this material lies on its low toxicity (Gombotz & Wee, 1998), film-forming ability and biodegradability (Benavides et al., 2012). Furthermore, the widely-recognised capacity of its sodium salt to form crosslinked networks in the presence of polyvalent cations, e.g. Ca^{2+}, has received greatest attention from the scientific community (Russo et al., 2007).

Within food applications, microencapsulation offers the possibility of customising the functionality of food products by incorporating active compounds that are protected from the environment and released within the matrix under controlled conditions (Soukoulis et al., 2017). Particularly, the use of alginate networks as encapsulating material for a range of phytochemicals, volatile additives, enzymes and probiotic bacteria has been intensively researched. For instance, Lupo et al. (2014) explored the use of alginate microbeads as carriers for cocoa polyphenols to offer alternatives to commercial synthetic antioxidants in foods, while Tan et al. (2018) investigated the stability of tocotrienols encapsulated in alginate–chitosan microcapsules, compared to non–encapsulated tocotrienols in bulk oil, during storage and in a food model system. Among the different phytochemicals, β-carotene is characterised by an extended hydrocarbon backbone and high degree of unsaturation, which leads to low water solubility, low bioaccessibility and poor chemical stability (Zhang et al., 2016). Its encapsulation has been the focus of numerous studies, given the potential health benefits as antioxidant and anti-inflammatory properties of this compound and the challenges linked to its incorporation in food products, many of which could be addressed by encapsulation. For instance, the entrapment of β-carotene into a delivery system could prevent its fast degradation while providing effective protection against oxidation (Soukoulis et al., 2017; Zhang et al., 2016).

The performance of calcium alginate networks as coatings and delivery systems tends to be defined by their thickness, porosity, permeability, mechanical strength and swelling behaviour. Some of these properties are significantly affected by the molecular structure of alginate as well as the kinetic governing the process of crosslinking. Several studies in literature have focused on exploring the performance of calcium alginate networks as coatings, where different crosslinking densities have been proposed by varying the concentration of cations (used

* Corresponding author.
E-mail addresses: joel.giron@usco.edu.co (J. Girón-Hernández), Piergiorgio.Gentile@newcastle.ac.uk (P. Gentile), Maria.Tinoco@northumbria.ac.uk (M. Benlloch-Tinoco).

https://doi.org/10.1016/j.carbpol.2021.118429
Received 2 March 2021; Received in revised form 4 July 2021; Accepted 8 July 2021
Available online 12 July 2021

as gelling agents) and the gelation time, or by comparing alginates with different amounts of guluronic fraction. For example, Li et al. (2015) investigated how concentration of $CaCl_2$ affected the gelation process and physical properties of calcium alginate films, while Russo et al. (2007) compared the mechanical properties and permeability of alginate matrices with different levels of crosslinking obtained by immersing alginate films with different ratios of guluronic acid on a 2% $CaCl_2$ aqueous solution. Furthermore, Patel et al. (2017) studied the effect of ionotropic gelation residence time on the crosslinking of alginate with $CaCl_2$ and their impact on the properties of alginate particles. However, little consideration has been made on the role that heterogeneity of the crosslinks may play on the capability of the matrix to limit the diffusion of molecules from the environment and, therefore, on the ability to minimise the degradation of the sensitive core materials. Externally gelled alginate systems tend to be heterogeneous with a gradient of zones that are crosslinked to different extents. While at the surface gel formation is instantaneous, there is a constant diffusion of Ca^{2+} towards the core, and of alginate from the core towards the gelled zone (Quong et al., 1998). Despite the crucial role that such heterogeneity could play on the barrier properties of the network, this is often overseen in the literature, while it is also implicitly assumed that similar alginate networks will be developed by using comparable amount of guluronic fraction and concentration of gelling agent. For instance, in one of the studies conducted by Zhang et al. (2016), addressing the physicochemical stability and bioaccessibility of β-carotene entrapped in alginate beads, the authors assumed preliminary that higher concentration of alginate should lead to enhanced chemical stability of β-carotene within the microparticles. However, their results did not confirm this.

The present study highlights the relevant role that heterogeneity of crosslinking plays on determining the barrier properties of alginate networks and aims at demonstrating that homogeneously crosslinked calcium alginate matrixes show an improved performance as carriers for β-carotene, since they allow for enhanced chemical stability of the core material. To this end, different concentrations of sodium alginate (0.25–2%) and calcium chloride (2.5–5%) were employed to develop a range of calcium alginate networks, in the form of films and beads, with different crosslinking densities. Finally, thickness, weight, solubility, swelling index, mechanical properties, calcium content, microstructure (SEM) and FTIR spectra of films were analysed, while the chemical stability of β-carotene over storage at 25, 35 and 45 °C when encapsulated in the calcium alginate beads was also evaluated.

2. Materials and methods

2.1. Materials

Sodium alginate (15–25 cP for 1% solution, Mw = 120,000–190,000 $g{\cdot}mol^{-1}$, M/G ratio = 1.56), calcium chloride (anhydrous granular ≤ 7.0 mm, ≥93%), sodium chloride (ACS reagent ≥99%), nitric acid (70% w/w), calcium (granular 99%), β-carotene (standard 97% purity) and all other chemicals were purchased from Sigma-Aldrich (UK). Deionised water was obtained throughout Milli-Q® Water Purification System (IQ 7005, Merk, UK).

2.2. Preparation of films and characterisation methods

2.2.1. Preparation of films

Films were prepared by solvent casting. Alginate (0.25, 0.5, 1, 1.5 and 2% w/v) was dissolved in deionised water by stirring on a hot plate at 60 °C and, then, sonicated in a heated bath (Bransonic® CPXH, Fisher Scientific, UK) (Chan et al., 2006; Zhang et al., 2016). When the solutions became completely clear, they were left to cool down for 24 h at room temperature and approximately 30 mg of each solution was poured onto a 60 mm diameter petri dish. Films were left to dry on a levelled surface at 37 °C for 60 h, and peeled off.

2.2.2. Preparation of crosslinked alginate films

Calcium alginate films were prepared by a dry-cast external gelation. The crosslinking solution was prepared by dissolving 2.5 and 5% w/v of $CaCl_2$ powder in deionised water (Li et al., 2016). Each dried sodium alginate film was immersed in 300 ml of crosslinking solution for 24 h, and then washed once with a solution of 4% w/v of NaCl and three times with deionised water to remove any surface unbound cations. The excess water was removed with a clean tissue paper, and, finally, the films were stored at room temperature and 65% relative humidity for 18 h before further use.

2.2.3. Determination of the thickness

Film thickness (t) was measured using a digital micrometer (IP65, Oxford Precision, UK). Six measurements were taken at the centre and around the perimeter of the film, for both alginate and crosslinked alginate films.

2.2.4. Apparent solubility and swelling index

Crosslinked samples were cut into square pieces of approximately 20 × 20 mm, weighted (w_o), immersed in 50 ml of distilled water and placed in a shaking water bath (Precision TSSWB15, ThermoScientific, UK) at 37 °C for 8 h. After this, the films were weighted (w_2). The apparent solubility (S_a) was calculated by the difference between the initial weight (w_o) and the weight (w_1) of the films dried at room temperature until constant weight was achieved, and expressed as a fraction of the initial weight. The swelling index (S_i) was calculated as:

$$S_i = \left(\frac{w_2 - w_0}{w_0}\right) \times 100 \quad (1)$$

where w_2 was the weight of the swelled filtered film and w_0 the initial weight. Five samples were analysed per condition.

2.2.5. Determination of the calcium content

The calcium content of the crosslinked films was determined by using a flame photometer (500 701, Jenway, UK), where the samples (round shape, 60 mm diameter) were placed into 20 ml of concentrated nitric acid (70% w/w) and heated for 10 min on a hot plate with stirring until reaching the boiling point. Once the films were completely dissolved, deionised water was added to the solutions up to 100 ml of final volume and then analysed (n = 4 per condition). A calibration curve with concentrations of calcium ranging from 10 to 100 ppm was calculated priorly. Calcium content was expressed as mg Ca per g of alginate.

2.2.6. Mechanical properties

The crosslinked and non crosslinked alginate films were cut in rectangular shape of 60 mm length (L) and 20 mm width (W). Model 3400 Instron (Instron Engineering Corporation, UK) was used to analyse the mechanical properties by setting the following operation conditions: initial grip separation of 50 mm and crosshead speed of 10 mm/min. The tensile strength (TS) was calculated by means of Eq. (2).

$$TS = \frac{F\,max}{A} \quad (2)$$

where F_{max} was the maximum load at breaking point, and A was the cross-sectional area calculated by multiplying the thickness (T) by the width (W). Elongation at break percentage [ε (%)] of the films was calculated using Eq. (3).

$$\varepsilon(\%) = \left(\frac{L_f - L_0}{L_0}\right) \times 100 \quad (3)$$

where L_f was the final length of the film at breakpoint and L_0 was the initial length of the film. Young's modulus (E) was calculated as the slope in the linear elastic region (0–5% of strain). At least five samples were analysed per condition.

Table 1
Weight (w_0), thickness (t), and Calcium content (Ca) of alginate-based films before and after crosslinking with $CaCl_2$.

Alginate (%)	Uncrosslinked		$CaCl_2$ (%)	Crosslinked		Δw_0 (%)	Δt (%)	Ca (mg/g alginate)
	w_0 (mg)	t (μm)		w_0 (mg)	t (μm)			
0.25	100.7 ± 5.9^{aA}	10.8 ± 1.9^{aA}	5	96.5 ± 2.6^{aA}	22.3 ± 2.2^{aB}	−4.2	106.6	174.7 ± 17.3^{a}
0.5	184.8 ± 30.0^{bA}	14.4 ± 2.2^{bA}		176.0 ± 13^{bA}	31.4 ± 2.3^{bB}	−4.7	118.5	93.7 ± 10.7^{b}
1	339.6 ± 12.9^{cA}	26.5 ± 2.1^{cA}		342.9 ± 2.3^{cB}	54.3 ± 0.7^{cB}	1.0	104.6	35.4 ± 1.3^{c}
1.5	471.5 ± 19.5^{dA}	40.7 ± 2.3^{dA}		481.4 ± 13.5^{dB}	78.5 ± 5.4^{dB}	2.1	92.8	13.5 ± 0.2^{d}
2	654.2 ± 22.9^{eA}	58.4 ± 2.4^{eA}		321.8 ± 8.8^{eA}	94.8 ± 3.6^{eB}	−0.4	62.4	8.9 ± 0.5^{e}
1	299.0 ± 13.1^{aA}	25.0 ± 2.2^{aB}	2.5	321.8 ± 8.8^{aB}	37.6 ± 2.0^{aB}	7.6	50.4	32.4 ± 0.9^{a}
2	696.8 ± 93.8^{bA}	58.1 ± 1.2^{bA}		697.2 ± 9.0^{bA}	89.6 ± 5.5^{bB}	0.1	54.2	7.4 ± 0.1^{b}

Different lowercase letters represent significant differences ($p < 0.05$) between the different alginate concentrations, while the different uppercase letters represent significant differences ($p < 0.05$) before and after crosslinking.

2.3. Preparation of calcium alginate beads and characterisation methods

2.3.1. Encapsulation of β-carotene in alginate beads

2.3.1.1. Preparation of oil-in-water (o/w) emulsion. Coarse β-carotene-loaded (0.01% w/w, Sigma-Aldrich, UK) o/w emulsions were prepared following the methodology described by Soukoulis et al. (2017). The droplet size in these coarse emulsions was further reduced using a homogeniser (T25 Ultra Turrax, IKA, UK) at 14,000 rpm for 5 min. These were used immediately after to prepare the alginate beads as described below.

2.3.1.2. Formation of alginate beads. Aqueous solutions containing different amounts of alginate (1 or 2% w/w) were prepared as described in Section 2.2.1. Alginate solutions and β-carotene-loaded emulsions were then mixed together (1:1 weight ratio) for 1 h with continuous stirring to form a mixture with 3% oil (w/w) and either 0.5 or 1% alginate (w/w). Then, externally crosslinked alginate beads were produced by extruding dropwise the β-carotene-loaded-alginate solution into 300 ml of 5% $CaCl_2$ under constant stirring. The beads were held in the $CaCl_2$ solution for 1 h at ambient temperature and under agitation to promote crosslinking. Finally, the alginate beads were collected by filtration and washed with deionised water and 4% NaCl to remove any excess ions from their surfaces. Subsequently, the beads were stored at 4 °C for 24 h to remove any residual external water, and final beads weight was determined. The encapsulation efficiency [*EE* (%)] was calculated using Eq. (4). As control, alginate beads that did not contain any β-carotene were prepared following a similar procedure.

$$EE(\%) = \frac{\beta - carotene\ in\ alginate\ beads}{Initial\ \beta - carotene\ content} \bullet 100 \quad (4)$$

2.3.2. Storage study

The β-carotene loaded alginate beads (0.5 and 1%) and β-carotene loaded bulk oil were stored in a controlled-temperature incubator at 25, 35 and 45 °C in darkness for a maximum of 32 days. Samples were withdrawn periodically every 4 days to analyse the content of β-carotene as described in the section below.

2.3.3. Extraction and quantification of β-carotene

β-carotene was isolated from the freshly made and stored alginate beads (0.5% and 1%) and bulk oil samples using a solvent extraction by adapting the method described by Biehler et al. (2010). Briefly, prior to the extraction, the alginate beads were dissolved with a saturated ethylenediaminetetraacetic acid (EDTA) solution to release the encapsulated β-carotene.

Since the samples only contained single carotenoids (β-carotene), quantification was done spectrophotometrically (Cary 50 UV–Vis, Agilent Technologies, UK). β-Carotene content in the samples (μg·100 g^{-1}) was calculated using the Beer–Lambert law (Eq. (5)).

$$A = \varepsilon_\lambda \cdot c \cdot d \quad (5)$$

where A is the measured absorbance, ε_λ the molar absorption coefficient of β-carotene in hexane at 453 nm (139,200 l·mol^{-1}· cm^{-1}) (Craft & Soares, 1992), c the molar concentration of β-carotene (mol/l), and d the width of the cuvette. As blank, Canola oil and alginate beads that did not contain any β-carotene were subjected to similar extraction procedures. All measurements were repeated three times.

2.3.4. Kinetic modelling of β-carotene degradation

To obtain the kinetic parameters explaining loss of β-carotene content in the bulk oil and alginate bead samples during storage, the amount of β-carotene detected in the samples was plotted vs. time at all temperatures studied. Zero, first and second order kinetics were hypothesized by applying the corresponding reaction rate expression. Then, the order that best fitted the experimental data (data not shown) was selected. Following this criterion, first-order kinetics (Eq. (6)) were used to describe degradation of β-carotene over time. The time for the concentration of a compound to fall to half its initial value (half-life, $t_{1/2}$) was also determined by Eq. (7).

$$ln\frac{C}{C_0} = -k \bullet t \quad (6)$$

$$t_{\frac{1}{2}} = \frac{\ln 2}{k} \quad (7)$$

where C represents the concentration (mg·100 g^{-1}) of the compound at the specific time t; C_0 the concentration (mg·100 g^{-1}) of each compound at time zero; and k the first-order constant ($days^{-1}$).

For all the measurements, best fit between the experimental and predicted data was assessed by means of the adjusted regression coefficient (R^2-ad.) (Eq. (8)), considering that the higher the R^2-ad. value the better the fit.

$$R^2 - ad. = \left[\frac{(m-1)\left(1 - \frac{SSQ_{REGRESSION}}{SSQ_{TOTAL}}\right)}{m-j}\right] \quad (8)$$

where m is the number of observations; j the number of model parameters and SSQ represents the sum of squares.

2.4. Statistical analysis

All the quantitative data were presented as mean ± standard deviation, unless noted otherwise. Furthermore, all variables were checked for normality. Analyses of variance by using ANOVA were used to test for significant differences among the used alginate concentrations and conditions for a given variable. Furthermore, Pearson correlation coefficients were used to quantify the association between pairs of variables. For the eight variables (w_0, t, TS, ε (%), E, S_a, S_i and Ca) group (n = 3 for each variable) of the crosslinked alginate films, a Principal Component Analysis (PCA) was performed. Statistical procedures were performed by using Statgraphics Centurion XVI (Statgraphics

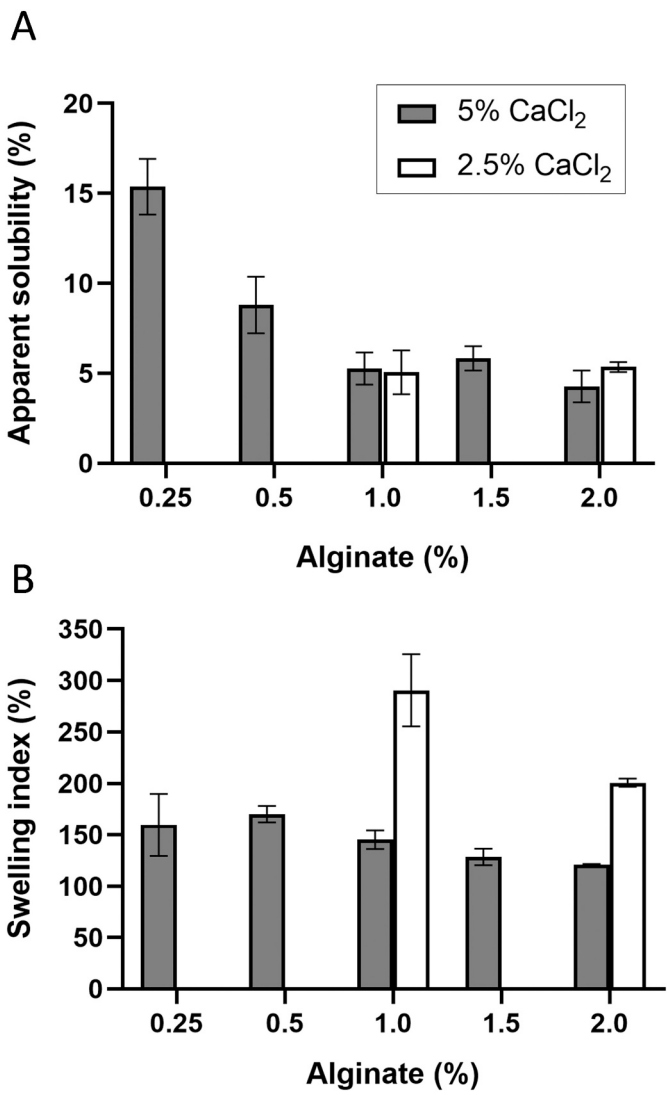

Fig. 1. (A) Apparent solubility and (B) swelling index of alginate-based films before and after crosslinking with $CaCl_2$.

Technologies, Inc. US).

3. Results and discussion

3.1. Characterisation of alginate films

3.1.1. Thickness, weight and calcium content

In this work thickness, weight and Calcium content were used as indicators of the microstructural characteristics of the alginate-based networks. Thickness, weight and Calcium content of the alginate films before and after crosslinking are shown in Table 1. Scanning Electronic Microscopy (SEM) with EDS analysis was also used to further explore microstructural changes in the samples linked to gelation (Supplementary material, Figs. S1, S2 and Table S1). Alginate films appeared very flexible and visually homogeneous with no brittle areas or bubbles. After crosslinking with 2.5 and 5% $CaCl_2$, the films increased significantly ($p < 0.05$) in thickness (50–119%) for all the studied concentrations of sodium alginate; nevertheless, no statistically significant changes ($p > 0.05$) on their weights were observed with no relevant loss of polymer during gelation. Similar ranges of values and observations on similar films before and after crosslinking have been widely reported in literature (Benavides et al., 2012; Chan et al., 2006). Gelation takes place when the alginate matrix is in a swollen (hydrated) state, since crosslinks increase the rigidity of the alginate chains, after drying they will keep occupying more space (Crossingham et al., 2014). However, they also experienced some shrinkage associated to the process of gelation due to chain aggregation, which tends to be more noticeable in densely and homogeneously crosslinked networks (Blandino et al., 1999; Chan et al., 2006).

The content of calcium in the crosslinked films (Table 1) was in the range of values reported in other studies for external gelation with similar concentrations of alginate and $CaCl_2$ (Li et al., 2015; Li et al., 2016; Takka & Acarturk, 1999). In our work, it was observed that at 5% $CaCl_2$ samples with lower alginate content (0.25% and 0.5%) showed higher calcium content, indicating significantly higher number of crosslinks ($p < 0.05$) (Table 1). This behaviour was in contrast with the results reported by other authors (Banerjee et al., 2009). Then, by increasing the alginate concentration, it was noticed a sharp decrease in values of calcium content for 1–2% alginate (35.4–8.9 mg Ca·g alginate^{-1}). FTIR spectra of the samples were also captured (Supplementary material, Fig. S3). As expected, the spectra showed a shift on the asymmetric -COO- and symmetric -COO- peaks after gelation, which was associated to the replacement of sodium ions by calcium ions. However, this shift was of similar magnitude for all the samples. As reported by Blandino et al. (1999), after instant crosslinking at the junction zones, the process of gel formation is controlled by the diffusion of Ca^{2+} across the chains of alginate, which then binds to the unoccupied binding sites on the polymer. Thus, at high concentrations of alginate, the diffusion of Ca^{2+} is considerably restricted due to the high levels of entanglement, and the majority of the crosslinks remains on the surface. Therefore, the obtained films can be considered highly heterogeneous crosslinked matrices. This hypothesis seems to be supported by SEM micrographs (Supplementary material, Fig. S1), as higher degree of heterogeneity was found in crosslinked samples with 1–2% alginate. Higher atomic concentration of calcium was also found in the surface of films with 1–2% of alginate (Supplementary material, Fig. S2 and Table S1).

3.1.2. Apparent solubility and swelling index

Apparent solubility and swelling index of calcium alginate films have been traditionally used as indicators of the extent of crosslinking (Li et al., 2015; Li et al., 2016; Rhim, 2004) and in the literature, lower solubility and swelling index have been assumed to be associated with higher crosslinking density. Fig. 1 reports solubility and swelling index values for the crosslinked samples. As control, uncrosslinked alginate films completely dissolved after 10 min of immersion in water, while the apparent solubility of crosslinked films ranged from 4.3 ± 0.9% to 15.4 ± 1.6% for films containing 2% and 0.25% of alginate respectively (Fig. 1(A)). These values were in good agreement with those reported in literature for samples with similar concentrations of alginate and $CaCl_2$ (Chan et al., 2006; Li et al., 2016). Furthermore, at 5% $CaCl_2$, films with higher concentration of alginate showed significantly lower values of apparent solubility and swelling index ($p < 0.05$), while a lower concentration of $CaCl_2$ (2.5%) led to a significant increase ($p < 0.05$) of the swelling index (Fig. 1(B)), without affecting the samples apparent solubility ($p > 0.05$). To be noticed, despite the lower swelling index at higher $CaCl_2$ concentration, the samples containing 1 and 2% alginate showed no differences in calcium content. This could indicate that, rather than the extent of crosslinking, the apparent solubility and the swelling index of the films were strongly affected by the distribution of the crosslinks. Particularly, the densely crosslinked surface of films containing 1–2% alginate may have simply restricted the absorption of water within the network and, therefore, limited the swelling and the loss of polymer chains through dissolution, as confirmed by the weight variation values (Table 1).

These results indicated that the concentration of alginate and crosslinking agent strongly affected the degree of swelling of the network and the density and heterogeneity of crosslinks. Therefore, it is also likely to impact on the performance of the network as encapsulating

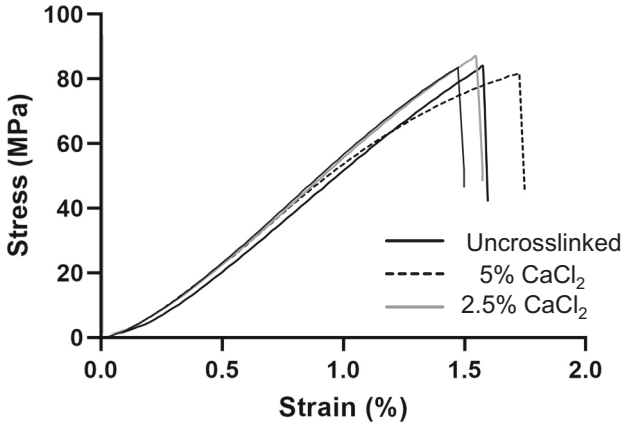

Fig. 2. Representative stress-strain curves for the 2% alginate-based films before and after crosslinking with $CaCl_2$.

material. In addition, the degree of swelling experienced by the alginate network during immersion in the gelling solution may also play a role in the behaviour of the matrix upon hydration, as indicated by the significant correlation found between the apparent solubility ($r = -0.701$) and swelling index ($r = -0.755$) and the thickness of the dry calcium alginate films ($p < 0.05$). A similar observation was reported by Li et al. (2015).

Consequently, all the studied properties of the calcium alginate networks need to be carefully considered when used in encapsulating applications, since their overall performance may be dramatically impacted by the heterogeneity of crosslinking and swelling degree.

3.1.3. Mechanical properties

Fig. 2 shows the representative stress-strain curves obtained for the 2% alginate film before and after crosslinking. Fig. 3 reports the values of the elongation (ε) and tensile strength (TS) at break and Elastic modulus (E) of the prepared films. Regarding the elongation at break, the crosslinked samples were characterised by higher values compared to the uncrosslinked films. As example, at 1% alginate content, crosslinked samples showed values of 1.73 ± 0.33% with 2.5% $CaCl_2$ and 3.17 ± 0.27% with 5% $CaCl_2$ while we evaluated an elongation at break of 1.01 ± 0.17% for the uncrosslinked samples.

Furthermore, it can be noticed that ε increased proportionally with the increase of alginate content for the uncrosslinked films, while after crosslinking the films presented a different trend. The highest ε values were found for the 0.5–1% alginate samples, with a significant decrease ($p < 0.05$) in the samples with higher alginate content (Fig. 3(A)).

For the tensile strength at break (Fig. 3(B)), the increase of alginate content led to higher values for both uncrosslinked and crosslinked conditions. Furthermore, we observed that films with 1.5% alginate crosslinked with 5% $CaCl_2$ showed the highest TS value (146.8 ± 10.9 MPa), indicating an increase of the resistance due to the reaction between alginate and Ca^{2+}, and consequently the formation of the "egg-box" structure. This behaviour is in agreement with published results (Costa et al., 2018).

Similarly, uncrosslinked samples showed higher values also for the elastic modulus. As example, we calculated 12,702.5 ± 1385.1 MPa and 2135.9 ± 748.0 MPa at 1% alginate for the uncrosslinked and 5% $CaCl_2$ crosslinked films, respectively. Furthermore, in all conditions, samples showed a similar behaviour for the elastic modulus (E) (Fig. 3(C)), reaching highest values at 1% and 1.5% alginate content for the uncrosslinked and crosslinked samples respectively, followed by a significant decrease ($p < 0.05$) at 2% alginate content. This was also confirmed in the E values calculated for the crosslinked samples at 2.5% $CaCl_2$. This trend was in accordance with similar works reported in literature (Cuadros et al., 2012).

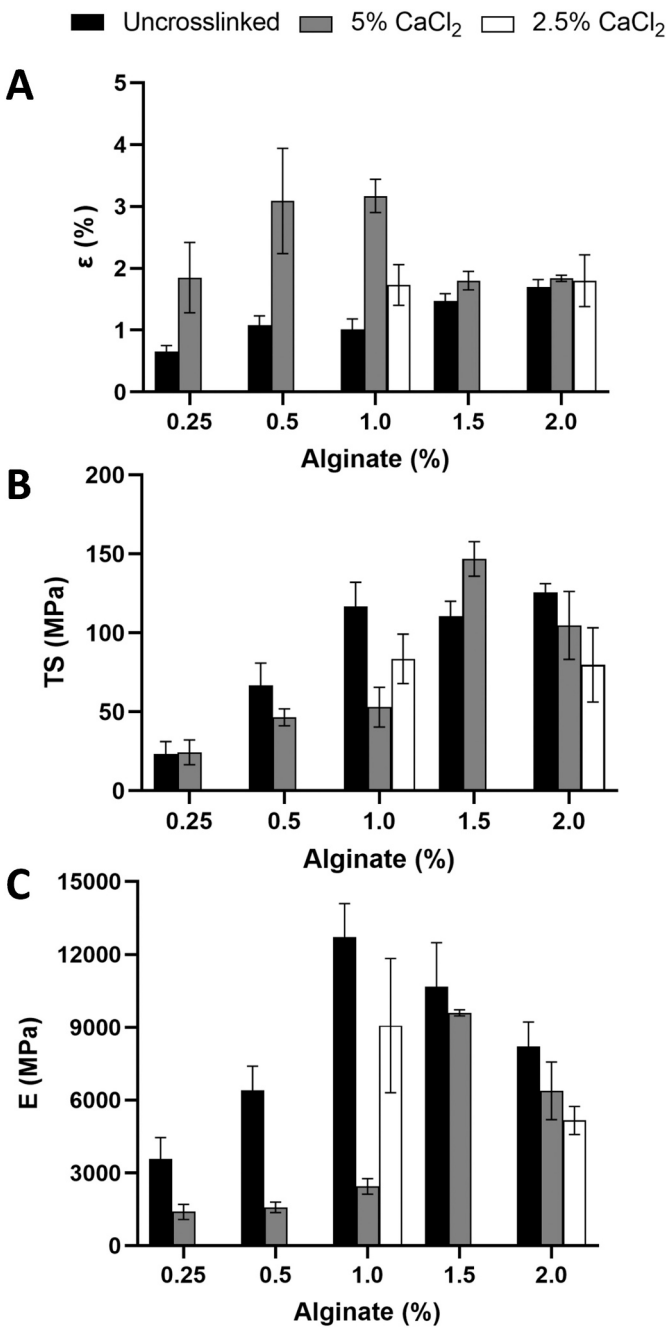

Fig. 3. Mechanical properties of alginate-based films before and after crosslinking with $CaCl_2$: elasticity at break (A), tensile strength at break (B) and Elastic modulus (C).

3.1.4. Multivariate analysis

PCA analysis of the characterisation variables was performed to determine whether the structural characteristics of the crosslinked films allowed discriminating between the different processing conditions. Fig. 4 shows the biplot used to assess the data structure and the loading of the first two components (PC1 and PC2), that explained 75.91% of the total variance. Particularly, calcium content (Ca) and apparent solubility (S_a) exhibited large positive loadings on PC1, that may be related with the crosslinked density, while the variables associated with the mechanical properties had equally a negative loading. For PC2 the elasticity [ε (%)] had the largest positive loading, while elastic modulus (E) and the hydration index (S_i) presented large negative loadings.

Furthermore, samples crosslinked with 2.5% $CaCl_2$ and the samples

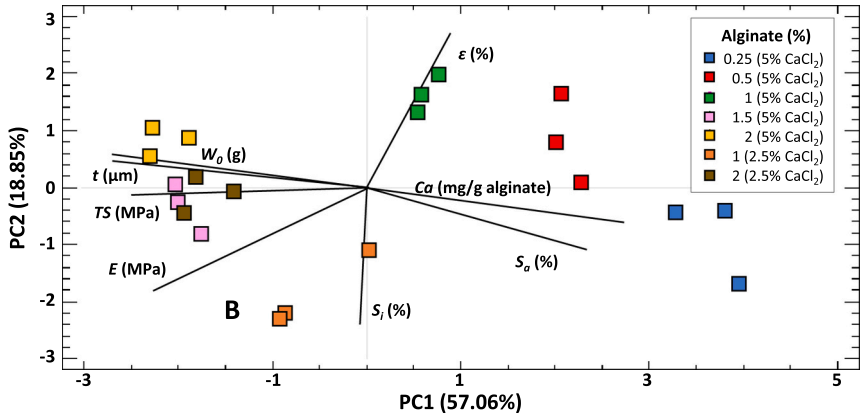

Fig. 4. Biplot (loading and score) obtained from the PCA of the crosslinking films.

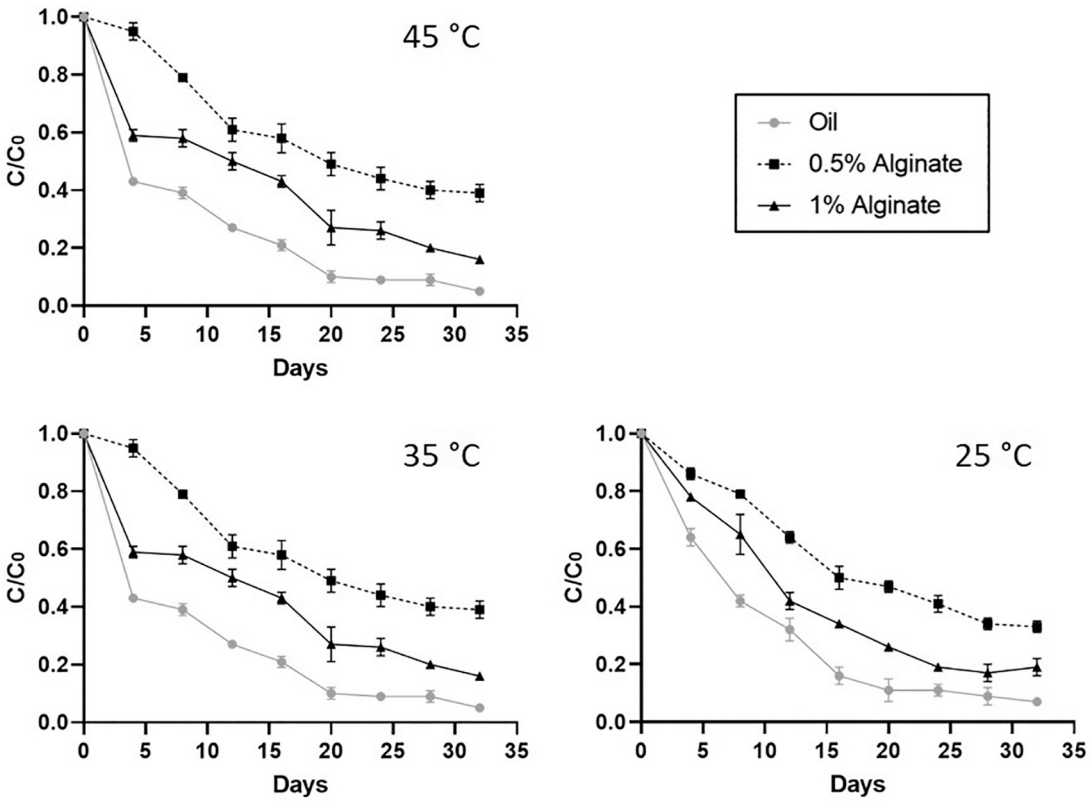

Fig. 5. β-Carotene retention (C/C_0) in bulk oil (●), 0.5% (■) and 1% (▲) alginate beads crosslinked at 5% $CaCl_2$ over storage at 45, 35 and 25 °C.

containing high concentration of alginate (>1.5%, 5% $CaCl_2$) were discriminated in the negative region of PC1 (57.06%) (Fig. 4), while the samples containing 0.5 and 1% alginate (5% $CaCl_2$) presented positive values for PC1. To be noticed, those samples were also located in the positive region of PC2 (18.85%). According to these results, those films, presenting similar and comparable characteristics, were selected for the further formation of the β-carotene loaded beads.

3.2. Degradation of β-carotene in alginate beads over storage

There is general interest in the use of carotenoids, such as β-carotene, as natural colorant and/or antioxidant in soft drinks, ice cream, yogurt drinks and other food applications in response to the increasing consumer concerns about the safety of synthetic components (Ravanfar et al., 2018; Toragall et al., 2020). In the present study, calcium alginate beads were loaded with β-carotene (EE (%) = 52.4% ± 4.5) to explore their protective role against degradation over storage at 25, 35 and 45 °C, when compared to β-carotene dissolved in bulk oil (Fig. 5). Calcium alginate beads with 0.5% and 1% sodium alginate (5% $CaCl_2$), with an average diameter of 0.10 ± 0.02 mm and 0.13 ± 0.03 mm respectively, were used to investigate the influence of the different extents and heterogeneity of crosslinking and mechanical properties of the networks on the chemical stability of β-carotene over storage.

As reported by other authors, β-carotene gradually degraded over time in all the samples, with higher storage temperatures leading to significantly ($p < 0.05$) faster degradation (Fig. 5). According to Gama and de Sylos (2007), the principal cause of carotenoid losses is oxidative degradation, which depends on the availability of oxygen, accelerated by heat, light, enzymes, metals, and co-oxidation with lipid hydroperoxides. To further investigate the protective role of the calcium alginate

Table 2
Half-life times ($t_{1/2}$: days), mean values and standard error of 3 independent replicates of the degradation rates (k: 100 $g \cdot mg^{-1} \cdot day^{-1}$) of β-carotene in oil, 0.5% and 1% calcium alginate beads during storage at 25, 35 and 45 °C. R^2-ad. is the adjusted regression coefficient.

Sample	T (°C)	$t_{1/2}$ (days)	k ($days^{-1}$)	R^2 ad.
Oil	25	8.03 ± 0.05aA	0.086 ± 0.004aA	0.948
	35	6.46 ± 0.07bA	0.106 ± 0.002bA	0.995
	45	3.69 ± 0.07cA	0.185 ± 0.021cA	0.876
0.5% alginate	25	21.89 ± 0.40aB	0.032 ± 0.002aB	0.939
	35	19.25 ± 1.66aB	0.037 ± 0.002aB	0.998
	45	10.89 ± 0.35bB	0.063 ± 0.005bB	0.928
1% alginate	25	13.00 ± 0.14aC	0.053 ± 0.003aC	0.946
	35	10.09 ± 0.09bC	0.068 ± 0.001bC	0.993
	45	5.58 ± 0.07cC	0.124 ± 0.009cC	0.946

Different lowercase letters represent significant differences ($p < 0.05$) between the different storage temperatures, while the different uppercase letters represent significant differences ($p < 0.05$) between different samples.

coatings, the kinetics of degradation of β-carotene in all the samples was studied (Table 2). Degradation of β-carotene was appropriately described by first-order kinetics and $t_{1/2}$ and k values were well within range of those reported in the literature (Benlloch-Tinoco et al., 2015).

Encapsulation significantly ($p < 0.05$) improved the chemical stability of β-carotene (Fig. 5). The degradation rate of β-carotene dispersed in bulk oil was at least 1.5 times higher than in any other sample. Larger differences were observed between oil and calcium alginate (0.5% and 1%) samples at higher storage temperatures (Table 2). Beads with 0.5% alginate were 1.5–2 times more efficient at preventing degradation of β-carotene than 1% calcium alginate beads ($p < 0.05$). This means that if β-carotene-loaded beads were to be stored at room temperature, for example, half of the β-carotene content would be degraded after 22 days for 0.5% alginate beads, compared to 13 days for 1% alginate beads. Similar observations have been reported by Zhang et al. (2016).

These results highlight that calcium alginate networks that are more extensively crosslinked (Table 1) and homogeneous in nature (Section 3.1.1), e.g. 0.5% alginate, are notably more efficient at protecting β-carotene from oxidation over storage. Firstly, diffusion of oxygen, which typically takes place directly through the polymeric matrix (capillary diffusion) and/or as a result of solubilisation in the film (activated diffusion) (Donhowe, 1994), may be restricted by the reduced macromolecular mobility associated with crosslinking. Alternatively, homogeneous networks, for being more flexible (lower elastic modulus, Fig. 3(C)), may experience a more uniform contraction during drying, which prevents excessive shrinkage, cracking and/or collapse, and therefore are able to restrict the diffusion of oxygen more efficiently than those that are stiffer (higher elastic modulus, Fig. 3(C)) and more heterogeneous (e.g. 1% alginate).

4. Conclusions

The high levels of entanglement typically found in uncrosslinked films with high concentrations of sodium alginate (≥1%) markedly effected the microstructural characteristics of the calcium alginate network formed upon crosslinking via external gelation with Ca^{2+}. When using $CaCl_2$ (≥2.5%) as gelling solution the extent of crosslinking in alginate films (≥1%) was highly limited by the heterogeneous nature of the network formed. Calcium alginate networks with a more homogeneous distribution of crosslinks (<1% alginate, 5% $CaCl_2$) showed more desirable physical and mechanical properties for encapsulation purposes, as indicated by their higher calcium content and elasticity. Improved barrier properties were also observed in more homogeneously and extensively crosslinked calcium alginate beads, as indicated by the enhanced chemical stability of β-carotene in 0.5% alginate samples. These findings highlight the need to adequately understand how crosslinking affects the microstructure of calcium alginate networks if their use as encapsulating material for food applications is to be exploited in an efficient and controlled manner.

CRediT authorship contribution statement

Joel Giron Hernandez: Investigation, Formal analysis, Writing - Reviewing and editing. **Piergiorgio Gentile:** Formal analysis, Writing - Reviewing and editing. **Maria Benlloch Tinoco:** Conceptualization, Methodology, Writing - Reviewing and editing, Funding acquisition.

Declaration of competing interest

None.

Acknowledgments

This study was supported financially by the Global Challenges Research Fund programme from Northumbria University.

Data availability

The data that support the findings of this study are available upon reasonable request to the corresponding author.

Appendix A. Supplementary data

Supplementary data to this article can be found online at https://doi.org/10.1016/j.carbpol.2021.118429.

References

Banerjee, A., Arha, M., Choudhary, S., Ashton, R. S., Bhatia, S. R., Schaffer, D. V., & Kane, R. S. (2009). The influence of hydrogel modulus on the proliferation and differentiation of encapsulated neural stem cells. *Biomaterials, 30*(27), 4695–4699.
Benavides, S., Villalobos-Carvajal, R., & Reyes, J. (2012). Physical, mechanical and antibacterial properties of alginate film: Effect of the crosslinking degree and oregano essential oil concentration. *Journal of Food Engineering, 110*(2), 232–239.
Benlloch-Tinoco, M., Kaulmann, A., Corte-Real, J., Rodrigo, D., Martínez-Navarrete, N., & Bohn, T. (2015). Chlorophylls and carotenoids of kiwifruit puree are affected similarly or less by microwave than by conventional heat processing and storage. *Food Chemistry, 187*, 254–262.
Biehler, E., Mayer, F., Hoffmann, L., Krause, E., & Bohn, T. (2010). Comparison of 3 spectrophotometric methods for carotenoid determination in frequently consumed fruits and vegetables. *Journal of Food Science, 75*(1), C55–C61.
Blandino, A., Macias, M., & Cantero, D. (1999). Formation of calcium alginate gel capsules: Influence of sodium alginate and CaCl2 concentration on gelation kinetics. *Journal of Bioscience and Bioengineering, 88*(6), 686–689.
Chan, L. W., Lee, H. Y., & Heng, P. W. (2006). Mechanisms of external and internal gelation and their impact on the functions of alginate as a coat and delivery system. *Carbohydrate Polymers, 63*(2), 176–187.
Costa, M. J., Marques, A. M., Pastrana, L. M., Teixeira, J. A., Sillankorva, S. M., & Cerqueira, M. A. (2018). Physicochemical properties of alginate-based films: Effect of ionic crosslinking and mannuronic and guluronic acid ratio. *Food Hydrocolloids, 81*, 442–448.
Craft, N. E., & Soares, J. H. (1992). Relative solubility, stability, and absorptivity of lutein and. beta.-carotene in organic solvents. *Journal of Agricultural and Food Chemistry, 40*(3), 431–434.
Crossingham, Y. J., Kerr, P. G., & Kennedy, R. A. (2014). Comparison of selected physico-chemical properties of calcium alginate films prepared by two different methods. *International Journal of Pharmaceutics, 473*(1–2), 259–269.
Cuadros, T. R., Skurtys, O., & Aguilera, J. M. (2012). Mechanical properties of calcium alginate fibers produced with a microfluidic device. *Carbohydrate Polymers, 89*(4), 1198–1206.
Donhowe, I. G. (1994). Edible films and coatings: Characteristics, formation, definitions, and testing methods. In *Edible coatings and films to improve food quality* (pp. 1–24).
Gama, J. J. T., & de Sylos, C. M. (2007). Effect of thermal pasteurization and concentration on carotenoid composition of Brazilian Valencia orange juice. *Food Chemistry, 100*(4), 1686–1690.
Gombotz, W. R., & Wee, S. (1998). Protein release from alginate matrices. *Advanced Drug Delivery Reviews, 31*(3), 267–285.
Li, J., He, J., Huang, Y., Li, D., & Chen, X. (2015). Improving surface and mechanical properties of alginate films by using ethanol as a co-solvent during external gelation. *Carbohydrate Polymers, 123*, 208–216.
Li, J., Wu, Y., He, J., & Huang, Y. (2016). A new insight to the effect of calcium concentration on gelation process and physical properties of alginate films. *Journal of Materials Science, 51*(12), 5791–5801.

Lupo, B., Maestro, A., Porras, M., Gutiérrez, J. M., & González, C. (2014). Preparation of alginate microspheres by emulsification/internal gelation to encapsulate cocoa polyphenols. *Food Hydrocolloids, 38*, 56–65.

Patel, M. A., AbouGhaly, M. H., Schryer-Praga, J. V., & Chadwick, K. (2017). The effect of ionotropic gelation residence time on alginate cross-linking and properties. *Carbohydrate Polymers, 155*, 362–371.

Quong, D., Neufeld, R., Skjåk-Bræk, G., & Poncelet, D. (1998). External versus internal source of calcium during the gelation of alginate beads for DNA encapsulation. *Biotechnology and Bioengineering, 57*(4), 438–446.

Ravanfar, R., Comunian, T. A., & Abbaspourrad, A. (2018). Thermoresponsive, water-dispersible microcapsules with a lipid-polysaccharide shell to protect heat-sensitive colorants. *Food Hydrocolloids, 81*, 419–428.

Rhim, J.-W. (2004). Physical and mechanical properties of water resistant sodium alginate films. *LWT - Food Science and Technology, 37*(3), 323–330.

Russo, R., Malinconico, M., & Santagata, G. (2007). Effect of cross-linking with calcium ions on the physical properties of alginate films. *Biomacromolecules, 8*(10), 3193–3197.

Soukoulis, C., Tsevdou, M., Andre, C. M., Cambier, S., Yonekura, L., Taoukis, P. S., & Hoffmann, L. (2017). Modulation of chemical stability and in vitro bioaccessibility of beta-carotene loaded in kappa-carrageenan oil-in-gel emulsions. *Food Chemistry, 220*, 208–218.

Takka, S., & Acarturk, F. (1999). Calcium alginate microparticles for oral administration: I: Effect of sodium alginate type on drug release and drug entrapment efficiency. *Journal of Microencapsulation, 16*(3), 275–290.

Tan, P. Y., Tan, T. B., Chang, H. W., Tey, B. T., Chan, E. S., Lai, O. M., … Tan, C. P. (2018). Effects of storage and yogurt matrix on the stability of tocotrienols encapsulated in chitosan-alginate microcapsules. *Food Chemistry, 241*, 79–85.

Toragall, V., Jayapala, N., & Vallikannan, B. (2020). Chitosan-oleic acid-sodium alginate a hybrid nanocarrier as an efficient delivery system for enhancement of lutein stability and bioavailability. *International Journal of Biological Macromolecules, 150*, 578–594.

Zhang, Z., Zhang, R., & McClements, D. J. (2016). Encapsulation of β-carotene in alginate-based hydrogel beads: Impact on physicochemical stability and bioaccessibility. *Food Hydrocolloids, 61*, 1–10.